Materials Science and Engineering C 77 (2017) 1044–1049

Contents lists available at ScienceDirect

Materials Science and Engineering C

journal homepage: www.elsevier.com/locate/msec

Antibiofilm effect of supramolecularly templated mesoporous silica coatings

Magdalena Pezzoni [a], Paolo N. Catalano [b], Ramón A. Pizarro [a], Martín F. Desimone [c], Galo J.A.A. Soler-Illia [d], Martín G. Bellino [b,*], Cristina S. Costa [a,*]

[a] Departamento de Radiobiología, Comisión Nacional de Energía Atómica, Av. General Paz 1499, B1650KNA San Martín, Argentina
[b] Departamento de Micro y Nanotecnología, Instituto de Nanociencia y Nanotecnología-Comisión Nacional de Energía Atómica-CONICET, Av. General Paz 1499, B1650KNA San Martín, Argentina
[c] Universidad de Buenos Aires, IQUIMEFA-CONICET, Facultad de Farmacia y Bioquímica, Junín 954, CP1113 Ciudad Autónoma de Buenos Aires, Argentina
[d] Instituto de Nanosistemas, Universidad Nacional de General San Martín, Av. 25 de Mayo 1021, B1650KNA San Martín, Argentina

ARTICLE INFO

Article history:
Received 24 February 2017
Received in revised form 29 March 2017
Accepted 1 April 2017
Available online 07 April 2017

Keywords:
Biofilms
Antibacterial
Transparent coating
Mesoporous thin film
Pseudomonas

ABSTRACT

Bacteria attached to solid surfaces and encased in a self-synthesized matrix, so-called biofilms, are highly difficult to eradicate and present negative impact on industry and human health. The ability of supramolecularly templated mesoporous silica coatings to inhibit biofilm formation in *Pseudomonas aeruginosa* is shown here. Assays employing submerged and air-liquid interface biofilms demonstrated that mesoporous coatings with tuned pore size significantly reduce the number of attached bacteria and matrix production. Given its versatility, scalability, robustness and low cost, our proposal is attractive for the production of transparent, inert and permanent antibiofilm coatings that could be applied on multiple surfaces.

1. Introduction

In nature, bacteria generally are not found as free cells but form complex structures attached to solid surfaces. In these structures, known as biofilms, bacteria grow embedded in a self-made matrix consisting of water and extracellular polymeric substances [1]. Biofilms have received great attention in the last years because of their enormous impact on industry and human health and their detrimental effects in economics and sanitary terms worldwide. They grow on industrial settings producing corrosion of pipelines and other facilities [2]. Biofilms also form on food-processing environments, water distribution systems and medical devices such as catheters, contact lenses and heart valves, with the consequent risk of a pathogenic process [3].

Bacterial biofilms have high resistance to antibiotics and other bactericidal agents compared to free cells [4]. In addition to conventional antimicrobial agents, alternatives approaches based on the use of nanotechnology (surfaces modification, nanomaterials) are intensely investigated to counteract bacterial biofilms [5–8]. It is widely accepted that the better way to combat biofilms is to prevent its formation instead of the use of chemical and physical treatments to eradicate them when they are installed [5]. Biofilm formation is a process that includes an initial phase of cell attachment, regulated by physical forces and hydrophobic interactions, and a subsequent phase of molecular-specific reactions between the cells and the surface leading to strong adhesion and proliferation [9]. The adhesion of microorganisms to surfaces not only depends on cell membrane properties and environmental factors, but also on the surface topography and roughness [9]. Taking this into account, controlling biofilm formation by tuning surfaces at nanoscale level is a major challenge in the development of antibiofilm strategies [5]. While it is usually accepted that surfaces with features smaller than bacterial cells inhibit bacterial attachment [10–15], the opposite effect was also described [16,17]. On the other hand, no difference between smooth and nanorough surfaces has been observed in sol-gel derived nanoporous TiO_2 deposited on titanium dental implant surfaces [18]. In this context, complex interplay among porosity, pore topology, roughness and hydrophobicity were observed in commercial titanium substrates assessed for bacterial attachment [19]. Moreover, a given surface can produce different effects depending on the microorganism tested [11]. Considering these controversies and the fact that these structures are usually obtained by difficult, expensive and delicate treatments, it is interesting to investigate new alternatives. In this regard, developing a simple and inexpensive method to cover a wide range of

Abbreviations: MOTFs, Mesoporous Oxide Thin Films; EISA, Evaporation-Induced Self Assembly; EEP, Ellipsometric Porosimetry; SEM, Scanning Electron Microscopy; TEM, Transmission Electron Microscopy; SAXS, Small Angle X-ray Scattering; NMS, non-mesoporous silica films; MS-4, mesoporous silica films with average pore diameter of ca. 4 nm; MS-9, mesoporous silica films with average pore diameter of ca. 9 nm; ALI, air-liquid interface; CFU, colony forming units; OD_{650}, optical density at 650 nm.

* Corresponding authors.
E-mail addresses: mbellino@cnea.gov.ar (M.G. Bellino), costa@cnea.gov.ar (C.S. Costa).

http://dx.doi.org/10.1016/j.msec.2017.04.022
0928-4931/

surfaces by highly controlled nanorough films would be very useful in the field of antibiofilm treatments.

Mesoporous Oxide Thin Films (MOTF) obtained by the so-called Evaporation-Induced Self Assembly (EISA) method have been applied in technologies such as catalysis, sorption, filtration, sensor devices and regulation of adhesion and proliferation of human osteoblastic cells [20–22]. MOTFs offer simplicity, low costs of production, nanostructural flexibility and robustness for the preparation of highly controlled nanoscale topographies. While anodized metal surfaces have demonstrated antibiofouling properties, their application is limited to conductive substrates. We took advantage of the straightforward and highly reproducible EISA thin film deposition and demonstrate in this work the possibility of utilizing mesoporous silica surfaces obtained by this technology to inhibit the biofilm formation of *Pseudomonas aeruginosa* (*P. aeruginosa*), a bacterium capable to form strong biofilms with enormous impact on medicine and industry [23,24]. Inhibition of biofilm formation through silica MOTFs has never been demonstrated before, and therefore, it is significant for the further development of antibiofilm transparent coatings on a variety of conductive or non-conductive substrates. In addition, this study contributes to the understanding of the influence of nanotopography on the formation of bacterial biofilms.

2. Experimental

2.1. Preparation and characterization of silica thin films

Glass substrates were dip-coated at 40–50% relative humidity (RH) and 1 mm s^{-1} withdrawal rates. $Si(OEt)_4$ (TEOS) was used as the inorganic precursor, and CTAB ($C_{16}H_{33}$–$N(CH_3)_3Br$) and Pluronics F127 ($HO(CH_2CH_2O)_{106}(CH_2CH(CH_3)O)_{70}$-$(CH_2CH_2O)_{106}OH$) (F127), were selected as the templates. TEOS was prehydrolyzed by refluxing for 1 h in a water/ethanol solution; $[H_2O]/[Si] = 1$; $[EtOH]/[TEOS] = 5$. Surfactant template, alcohol, and acidic water were added to the prehydrolyzed solution in order to prepare the precursor solutions, with final composition TEOS:EtOH:H_2O (0.1 M HCl):CTAB equal to 1:40:5:0.1 molar ratio or TEOS:EtOH:H_2O (0.1 M HCl):F127 equal to 1:40:5:0.0075 molar ratio. After deposition by dip-coating, the films were placed in a 50% RH chamber for 24 h. The films were then subjected to a consolidation thermal treatment, which consisted of heating at 60 °C for 24 h and at 130 °C for another 24 h. Finally, the films were calcined at 350 °C for 2 h in order to remove the template. For comparison, nonporous films were made as described, but in the absence of the polymeric template. Film thickness were obtained from the ellipsometric parameters ψ and Δ at each P/Ps (Ps being the saturation water pressure), which was varied from 0 to 1 using a SOPRA GES5A apparatus, equipped with microspot optics. Pore size distributions of mesoporous films were obtained from water adsorption–desorption isotherms determined by Ellipsometric Porosimetry (EEP) according to current protocols [25]. Film porosity was evaluated by the WinElli 2 software (SopraInc), which transforms the variation of n with P/Ps into filled pore volume by using a three-medium BEMA treatment. Pore and neck size distributions are derived according to a Kelvin model. Contact angles were determined by averaging measurements on five distilled water droplets using a Ramé-Hart 290 contact-angle apparatus. Micrographs were obtained using a Philips EM 301 TEM operating at 60 kV.

2.2. Bacterial strain and growth conditions

The study was conducted using the prototypical *P. aeruginosa* strain PAO1 (B. W. Holloway). Bacterial cultures were grown at 37 °C in complete LB broth (10 g tryptone, 5 g yeast extract and 5 g NaCl bring the volume up to 1000 mL in distilled water); for growth in solid medium, 15 g L^{-1} agar were added.

2.3. Biofilm formation

Control and mesoporous slides employed in biofilm assays were 20 mm × 25 mm × 1 mm; they were sterilized by soaking in ethanol 70% and subsequent evaporation at 60 °C before use in biological assays. For the formation of submerged biofilms, slides were placed horizontally at the bottom of 100 mL glass beakers and covered by 10 mL of overnight cultures diluted to an optical density at 650 nm (OD_{650}) of 0.01 in LB. For air-liquid interface (ALI) systems, the slides were placed vertically at the bottom of 50 mL Falcon tubes and covered by 5 mL of overnight cultures diluted to an OD_{650} of 0.01 in LB so that about half of the slide was submerged. The beakers and tubes were capped with cotton plugs and incubated at 37 °C for 4, 8 or 24 h without shaking.

2.4. Biofilm quantification

The number of viable cells on the slides was evaluated by counting the number of colony forming units (CFU) on LB plates [26]. To this end, glasses containing the biofilms were removed at the indicated times (4, 8 or 24 h) and washed with distilled sterile water to eliminate unattached cells. The bacterial biomass was scraped from the glass with a sterile plastic spatula and homogenized by vigorous vortexing in NaCl 0.1 M. Appropriate dilutions of these suspensions were spread onto LB solid medium and the colonies were counted after 24 h incubation at 37 °C. Total biofilm mass on test and control surfaces was evaluated by the crystal violet stain method [27]. To this purpose, slides carrying 24 h old biofilms were washed with distilled water to remove unattached cells and stained with 0.1% (wt vol^{-1}) crystal violet solution for 30 min. The slides were washed and the crystal violet attached to the slides was dissolved in a mixture of 96% ethanol and 30% acetic acid (1:1). Absorbance at 575 nm was measured in the resulting solution. A set of slides carrying 24 h old biofilms stained with crystal violet was photographed to illustrate the effect of mesoporous surfaces on biofilm formation. Matrix fractionation and quantification of extracellular polymeric substances (polysaccharides, proteins and DNA) present in this compartment was based on protocols employed in the laboratory [26]. To this end, slides carrying 24 h old biofilms were removed from the glass beakers and washed once with distilled water. The biofilms were carefully scraped from the glass surfaces and suspended in 0.1 M NaCl. The cells were dispersed by vigorous stirring for 5 min at room temperature and then separated by centrifugation for 30 min at 4 °C. The absence of cells in the supernatant (matrix fraction) was confirmed by plating on solid LB medium. The viable cell number obtained in the cell fraction was similar to that observed in biofilm assays without matrix separation, indicating that no significant cell lysis was generated by the procedure. Content of polysaccharides, proteins and DNA was then evaluated in the matrix fraction. Polysaccharides content was determined by the phenol/sulfuric acid method, using glucose as standard [28]. Protein content was determined by the Lowry's method, using bovine albumin as standard [29]. Extracellular DNA was quantified by evaluating the absorbance at 260–280 nm using a Nanodrop 2000 (Thermo Scientific NanoDrop).

2.5. Scanning Electron Microscopy (SEM) images

24 h biofilms were fixed in 2.5% glutaraldehyde for 2 h, washed with MilliQ water and dehydrated in a graded ethanol series (75%, 96%, 100%). Then, they were dried, sputter-coated with gold and examined by SEM. SEM images were obtained using a SUPRA 40 (Carl Zeiss AG) microscopy.

2.6. Statistical analysis

All samples were analyzed at least in triplicate. Data are represented as means ± SE. Statistical significance was assessed by Student's *t*-test; $p < 0.05$ was considered statistically significant.

3. Results and discussion

3.1. Synthesis and characterization of nanostructured silica coatings

The EISA method was used to build a set of silica thin films with different mesoporous structures on standard microscope glass slides, as described previously [22,30]. Transparent and crack-free films were deposited by dip-coating using the supramolecularly templated partially hydrolyzed oxide precursor $Si(OEt)_4$ (TEOS). CTAB and Pluronics F127 were chosen as surfactants to attain different lyotropic mesophases in order to create surfaces with different pore sizes and symmetries after removal of the template. Control surfaces were non-nanoporous silica films (hereafter NMS), which were synthesized by the same procedure described above but without the surfactant template. EEP of mesoporous films (Fig. 1) showed a large pore volume (37–40%) and uniform pore size estimated from the adsorption branch. In the case of CTAB-templated films with a 3D hexagonal mesostructure, an average pore diameter of ca. 4 nm was obtained (hereafter MS-4). Larger pore diameters were obtained in the case of Pluronics F127, resulting in a cubic, 9 nm pore diameter mesostructure (hereafter MS-9). These differences in mesoporous structure are illustrated in their respective Transmission Electron Microscopy (TEM) images inserted in Fig. 1 and Small Angle X-ray Scattering (SAXS) patterns showed in the Supplementary data (Fig. S1). The structural features and contact angle measurements of the different films utilized are summarized in Table 1 [22,30]. Contact angle values indicated that all the surfaces were hydrophilic, with the mesoporous surface MS-4 presenting relatively higher hydrophilicity than NMS and MS-9 films.

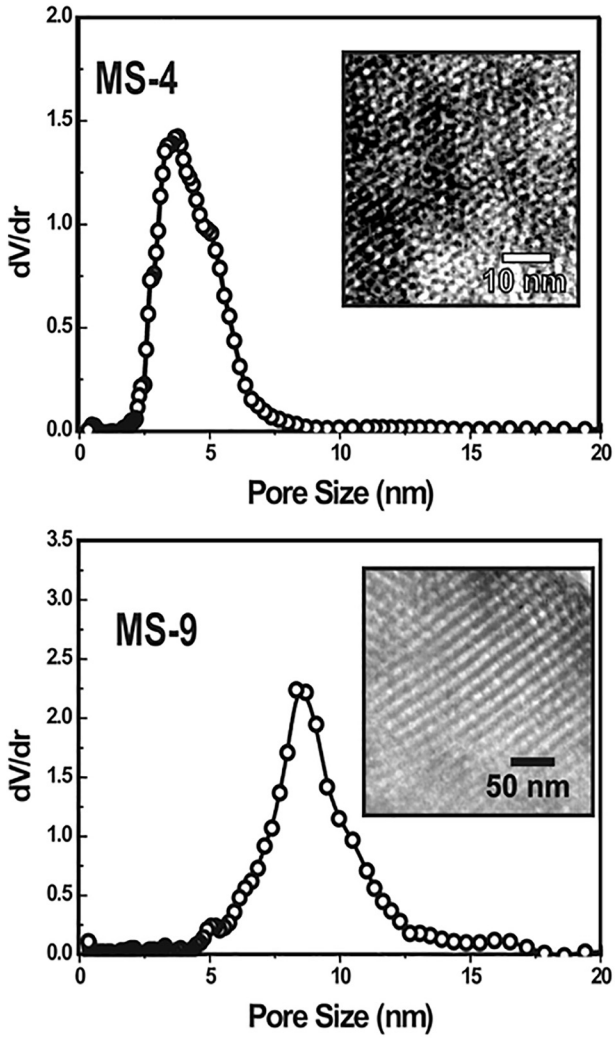

Fig. 1. Pore size distribution of mesoporous films employed in this study. The pore size distribution was obtained by water adsorption-desorption isotherms at 298 K. TEM images of the mesoporous films are shown as inserts. MS-4 and MS-9 refers to films with average pore diameter of ca. 4 nm and 9 nm, respectively.

Table 1
Structural data and contact angle measurements of the films employed in this study.

Film type	Pore size (nm)	Porosity (%)	Thickness (nm)	Contact angle (°)
NMS	–	5 ± 0.5	93 ± 1	23.0 ± 1
MS-4	4.1 ± 0.5	42 ± 2	150 ± 1	16.0 ± 1
MS-9	9.2 ± 0.8	37 ± 2	100 ± 1	28.0 ± 2

3.2. Antibiofilm effect of nanostructured silica coatings

In order to analyze the effect of mesoporous silica coatings on biofilm formation, static systems instead of continuous flow methods were employed because they are useful for examining early events in biofilm formation [27]. Two types of assays were performed: submerged, where the surfaces remained completely covered by the cell suspension, and ALI, where only about half of the surfaces were covered. In submerged assays, the biofilm grows in patches on the entire surface, while in ALI assays, the biofilm forms preferentially at the air-liquid interface. It is worth to mention that submerged systems are the most commonly used in biofilms studies. On the other hand, studies with ALI systems are relevant for industrial and piping facilities because these structures are partly filled with liquids during operation [31]. The assays were conducted with *P. aeruginosa*, a microorganism largely employed as model in biofilm studies. This microorganism is a versatile bacterium present in aquatic and terrestrial environments and a relevant opportunistic pathogen of humans.

Fig. 2 shows the effect of nanoporous silica coatings on the number of viable cells (CFU) in 4, 8 and 24 h old biofilms. The viable cell count after 4 h incubation showed no significant difference between nanoporous and smooth surfaces in both submerged and ALI systems. However, after 8 h incubation, the number of adhered cells to MS-4 and MS-9 in submerged systems was significantly lower ($p < 0.01$) compared to smooth surfaces, although no difference was observed between both nanostructured films. In ALI systems, a significant decrease on cell adhesion ($p < 0.05$) was observed only in MS-9 films, where the number of adhered cells decreased 4-fold compared to smooth surfaces. The analysis of mature biofilms was performed on 24 h old biofilms because biofilms cultured for longer times produced equal or lower biomass in our conditions. In both systems, less viable cells were recovered from nanoporous surfaces compared to smooth surfaces, especially in the case of MS-9, where the number of adhered cells was about 3-fold lower than in NMS films ($p < 0.05$ for submerged assays; $p < 0.003$ for ALI assays). In both assays a significant ($p < 0.05$) lower viable cell count was observed in MS-9 compared to MS-4. These results indicate that nanoporous silica coatings inhibit proliferation of biofilm cells, especially in the case of MS-9 films.

The whole biofilm mass in control and in test surfaces was evaluated by staining with crystal violet, a dye commonly used to visualize and quantify biofilms which not only stains cells but any biological material adhering to the surface. Representative images of stained 24 h biofilms clearly demonstrate the inhibitory effect of mesoporous coatings on biofilm formation (Fig. 3). Quantification of crystal violet adhered to the surfaces by measuring its absorbance at 575 nm supported this observation. A significant decrease in A_{575} was observed in MS-4 ($p < 0.05$) and MS-9 ($p < 0.01$) compared to NMS films, and in MS-9 compared to MS-4 ($p < 0.03$), both in submerged and ALI systems (Fig. 3).

Extracellular polymeric substances such as polysaccharides, proteins and DNA present in biofilm matrix are essential in providing mechanical stability and architecture to biofilm, adhesion to surfaces, and

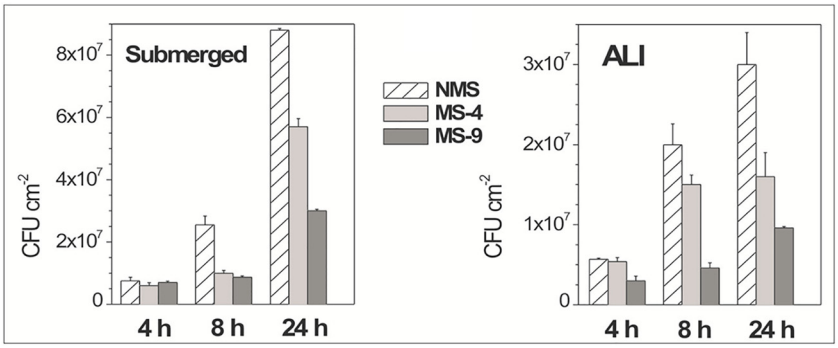

Fig. 2. Effect of mesoporous surfaces on the average numbers of attached cells. Submerged and ALI biofilms were grown on mesoporous MS-4 and MS-9 surfaces; non-mesoporous surfaces (NMS) were assessed as control. After 4, 8 and 24 h incubation at 37 °C, the number of viable cells attached to the different surfaces was quantified by the plate count method.

protection of bacterial cells against diverse stress factors [32]. Therefore, the effect of surface nanotopography on the concentration of these compounds was evaluated in 24 h old biofilms. As shown in Fig. 4, a slight decrease of polysaccharides and proteins levels was observed in submerged biofilms formed on nanoporous surfaces compared to control surfaces, but these differences were not significant. On the contrary, a significant decrease of polysaccharides, proteins and DNA levels was observed in ALI biofilms grown on nanoporous films ($p < 0.05$ between NMS and MS-4 or MS-9), following the same trend observed for the viable cell count. It should be noted the higher level of extracellular polysaccharides observed in ALI biofilms compared to submerged biofilms (Fig. 4).

Fig. 5 shows representative SEM images of 24 h biofilms grown on nanostructured and control surfaces. No specific attachment sites were observed. Based on a recent work suggesting that bacteria respond to the topography by maximizing its contact area with the surface, this was an expected result, since the pores are uniformly distributed and the distance between them is much smaller than the bacterium's length (2–3 μm) so that the cells would be unable to be placed preferentially in smooth areas between the pores [10]. The trend of bacterial attachment observed in SEM images was similar to that observed in Fig. 2, that is NMS > MS-4 > MS-9.

Additional assays employing conventional glass slides without coating were also performed as control. The obtained values for crystal violet staining, CFU cm^{-2} and extracelllular polymeric substances quantification were similar or even higher than those obtained for NMS surfaces, supporting the practical antibiofilm application of MOTFs (data not shown).

Taken as a whole, the results presented in this study indicate that the mesoporous silica coatings described here inhibit the formation of bacterial biofilms with respect to non-mesoporous silica films. Moreover, MS-9 films had a greater effect compared to MS-4 films, suggesting that the increase of pore size and/or the different arrangement of pores significantly decrease the number of attached bacteria and matrix production. In addition to surface topography, hydrophobicity also influences bacterial adhesion and proliferation [9]. It has been suggested that hydrophobic surfaces are more susceptible to adhesion than hydrophilic ones [33]. In the particular case of *P. aeruginosa*, it was demonstrated that adhesion to a variety of glass and metal-oxide surfaces is greater as hydrophobicity increases [34]. In this study, the hydrophobic character of the surfaces did not correlate with biofilm formation. Despite being slightly more hydrophilic, MS-4 films allowed higher biofilm development compared to MS-9 films, suggesting that indeed the nanotopography is the key factor in the phenomenon reported in this work. In order to investigate the mechanisms involved in the effect of nanostructured surfaces on bacterial attachment, it was demonstrated in *Escherichia coli* that nanorough substrates modify the expression of genes involved in fimbrial synthesis (organelles related to cell adhesion) and stress response [35,36]. On the other hand, studies in *P. fluorescens* demonstrated that bacterial assemblages involved in colonization of nanostructured surfaces are disorganized [37] and motility strategies (flagella orientation, elongation, aggregation in rafts) responsible of bacterial spreading are affected by micropatterns [16]. Other study on the effect of micro and nanoscale topography on bacterial adhesion revealed that bacterial cells exhibit different morphologies and different number and size of appendages involved in attachment, depending on the topographical structure of the surface [11]. In summary, it is probably that the effect of mesoporous silica on cell adhesion and proliferation obeys to genetic, proteomic and morphological changes in response to mechanical stress.

To the best of our knowledge, our results on the effect of nanoscale topography on the matrix components are interesting, since

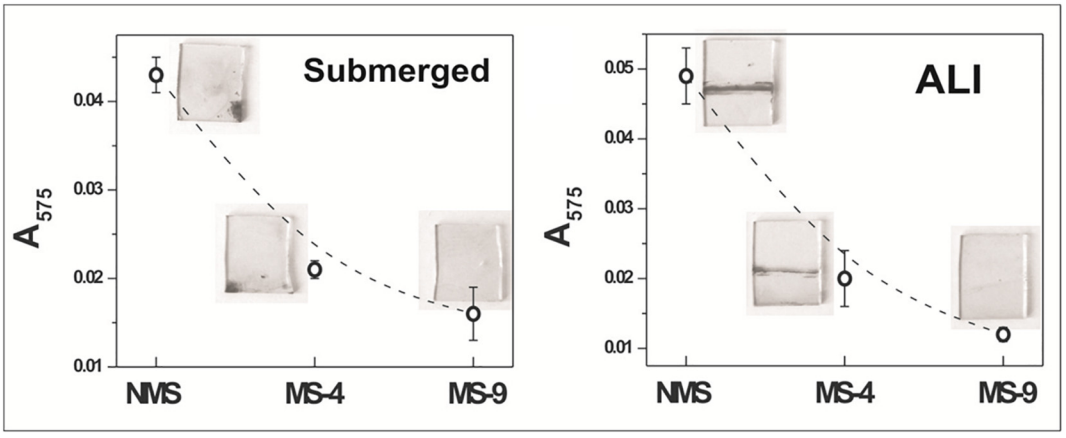

Fig. 3. Effect of mesoporous surfaces on the formation of biofilm assessed by crystal violet staining. Images depict crystal violet stained submerged and ALI biofilms grown on NMS, MS-4 and MS-9 films for 24 h. Crystal violet attached to the slides was quantified by measuring absorbance at 575 nm.

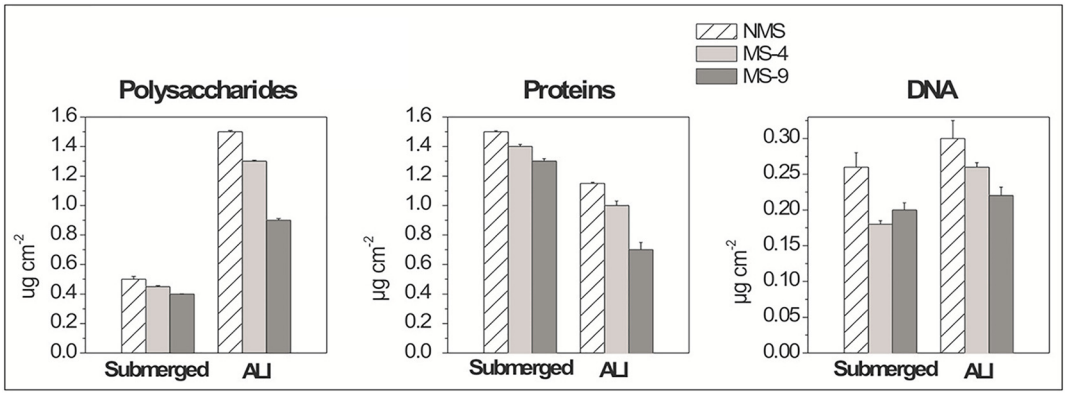

Fig. 4. Effect of mesoporous surfaces on the composition of biofilm matrices. Submerged and ALI biofilms were grown on NMS, MS-4 and MS-9 surfaces. After 24 h incubation at 37 °C, extracellular polymeric substances (polysaccharides, proteins and DNA) were quantified.

quantitative studies on the role of nanotopography on biofilm formation are usually based on microscopic counting of adherent bacteria, CFU plate counts and general methods as thickness or density measurements [9]. ALI biofilms grown on nanostructured surfaces showed a significant decrease in the levels of matrix components compared to smooth films. On the contrary, this difference was not as evident in submerged systems, indicating that the effect of nanotopography on matrix formation is stronger under aerobiosis, at least under the conditions employed in this study.

Although several types of nanostructured surfaces with antibiofilm properties have been described, the most significant difference with our proposal is that they are mostly obtained by modification of pre-existing surfaces, not by covering it, which demonstrates the high versatility of MOTFs. Hu et al. prepared superhydrophobic nanorough polymer coatings by electrospraying, but due to the biodegradability of the polymer, this method provides a temporary anti-adhesion [38]. In addition, to the best of our knowledge, most nanorough surfaces described are not scalable, they are substrate-limited (e.g., to conductive surfaces in the case of anodized oxides), non-robust (e.g., fiber-coated surfaces), and sometimes require high cost materials and specific facilities of micromanufacturing [11,13,15], which increases the costs and scalability. Other nanostructured surfaces are even more complex, for example those requiring the use of ultraviolet radiation and/or the additional use of antibacterial substances [39,40], some of them potentially toxic to human tissues [39]. In addition to our proposal, mesoporous silica has been employed to obtain nanocomposites for other potential biomedical applications, such as drug delivery against cancer and other diseases [41–45].

From a practical point of view, the inhibitory effect of mesoporous silica coatings on biofilm formation described in this work can be particularly attractive for the production of robust, inert, permanent and transparent antibacterial coatings that could be used on a variety of substrates in diverse applications, for example, in pipelines, biomedical and food facilities. Future studies testing the effect of these coatings on other microorganisms and natural occurring biofilms should be carried out in a systematic way in order to further broaden the research on their usefulness.

4. Conclusions

In this work, we demonstrate, for the first time, the ability of MOTF to inhibit biofilm formation in *P. aeruginosa*, a bacterium capable to form robust biofilms with enormous impact on medicine and industry. Mesoporous films not only inhibited cell proliferation but also biofilm matrix production, a quite novel and relevant result given the essential role of this compartment in providing mechanical stability and protection against antibacterial agents. Compared to previous approaches of nanorough surfaces synthesis, MOTF preparation is simple and flexible on potentially any surface, the precursors are accessible molecules and the performance is clearly superior, obtaining ordered and highly

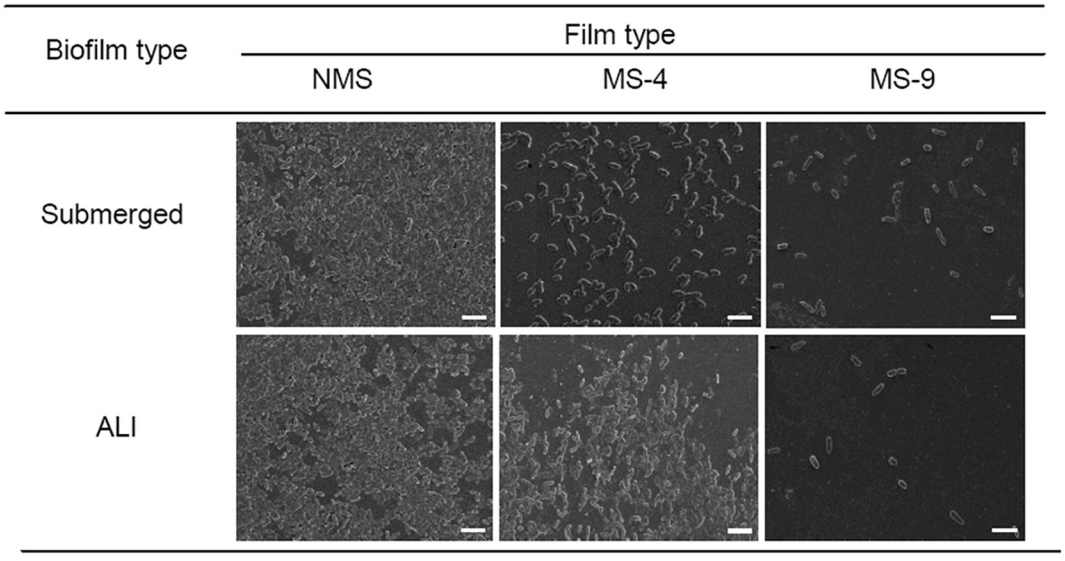

Fig. 5. SEM images of 24 h biofilms grown on NMS, MS-4 and MS-9 films. The bar represents 5 µm.

reproducible films. These robust, inert, permanent and transparent antibacterial coatings could be used in diverse surfaces in the biomedical, biotechnology and industrial fields.

Supplementary data to this article can be found online at http://dx.doi.org/10.1016/j.msec.2017.04.022.

Acknowledgments

This work was supported by CNEA, Consejo Nacional de Investigaciones Científicas y Técnicas (PIP 00186) and Agencia Nacional de Promoción Científica y Tecnológica (PICT 2969, PICT 2087). M.P., M.G.B., P.C., M.F.D. and G.J.A.A.S.-I. are staff members of Consejo Nacional de Investigaciones Científicas y Técnicas.

References

[1] J.W. Costerton, Z. Lewandowski, D.E. Caldwell, D.R. Korber, H.M. Lappin-Scott, Microbial biofilms, Annu. Rev. Microbiol. 49 (1995) 711–745.
[2] A. Rajasekar, B. Anandkumar, S. Maruthamuthu, Y.P. Ting, P.K.S.M. Rahman, Characterization of corrosive bacterial consortia isolated from petroleum-product-transporting pipelines, Appl. Microbiol. Biotechnol. 85 (2010) 1175–1188.
[3] P. Gupta, S. Sarkar, B. Das, S. Bhattacharjee, P. Tribedi, Biofilm, pathogenesis and prevention-a journey to break the wall: a review, Arch. Microbiol. 198 (2016) 1–15.
[4] T.-F.C. Mah, G.A. O'Toole, Mechanisms of biofilm resistance to antimicrobial agents, Trends Microbiol. 9 (2001) 34–39.
[5] L. Rizzello, R. Cingolani, P.P. Pompa, Nanotechnology tools for antibacterial materials, Nanomedicine (London) 8 (2013) 807–821.
[6] R.K. Kasimanickam, A. Ranjan, G.V. Asokan, V.R. Kasimanickam, J.P. Kastelic, Prevention and treatment of biofilms by hybrid- and nanotechnologies, Int. J. Nanomedicine 8 (2013) 2089–2819.
[7] B. Snoddy, A.C. Jayasuriya, The use of nanomaterials to treat bone infections, Mater. Sci. Eng. C 67 (2016) 822–833.
[8] M. Samiei, A. Farjami, S.M. Dizaj, F. Lotfipour, Nanoparticles for antimicrobial purposes in endodontics: a systematic review of in vitro studies, Mater. Sci. Eng. C 58 (2016) 1269–1278.
[9] M. Katsikogianni, Y.F. Missirlis, Concise review of mechanisms of bacterial adhesion to biomaterials and of techniques used in estimating bacteria-material interactions, Eur. Cell. Mater. 8 (2004) 37–57.
[10] A.V. Sing, V. Vyas, R. Patil, V. Sharma, P.E. Scopelliti, G. Bongiorno, A. Podestà, C. Lenardi, W.N. Gade, P. Milani, Quantitative characterization of the influence of the nanoscale morphology of nanostructured surfaces on bacterial adhesion and biofilm formation, PLoS ONE 6 (2011), e25029. .
[11] L.C. Hsu, J. Fang, D.A. Borca-Tasciuc, R.W. Worobo, C.I. Moraru, Effect of micro and nanoscale topography on the adhesion of bacterial cells to solid surfaces, Appl. Environ. Microbiol. 79 (2013) 2703–2712.
[12] M. Kargar, J. Wang, A.S. Nain, B. Behkam, Controlling bacterial adhesion to surfaces using topographical cues: a study of the interaction of *Pseudomonas aeruginosa* with nanofiber-textured surfaces, Soft Matter 8 (2012) 10254–10259.
[13] G. Feng, Y. Cheng, S.-Y. Wang, L.C. Hsu, Y. Feliz, D.A. Borca-Tasciuc, R.W. Worobo, C.I. Moraru, Alumina surfaces with nanoscale topography reduce attachment and biofilm formation by *Escherichia coli* and *Listeria* spp, Biofouling 30 (2014) 1253–1268.
[14] M.R. Park, M.K. Banks, B. Applegate, T.J. Webster, Influence of nanophase titania topography on bacterial attachment and metabolism, Int. J. Nanomedicine 3 (2008) 497–504.
[15] N. Mitik-Dineva, J. Wang, V.K. Truong, P. Stoddart, F. Malherbe, R.J. Crawford, E.P. Ivanova, *Escherichia coli*, *Pseudomonas aeruginosa*, and *Staphylococcus aureus* attachment patterns on glass surfaces with nanoscale roughness, Curr. Microbiol. 58 (2009) 268–273.
[16] C. Diaz, P.L. Schilardi, P.C. dos Santos Claro, R.C. Salvarezza, M.A. Fernandez Lorenzo de Mele, Submicron trenches reduce the *Pseudomonas fluorescens* colonization rate on solid surfaces, ACS Appl. Mater. Interfaces 1 (2009) 136–143.
[17] S.D. Puckett, E. Taylor, T. Raimondo, T.J. Webster, The relationship between the nanostructure of titanium surfaces and bacterial attachment, Biomaterials 31 (2010) 706–713.
[18] V. Fröjd, P. Linderbäck, A. Wennerberg, L. Chávez de Paz, G. Svensäter, J.R. Davies, Effect of nanoporous TiO_2 coating and anodized Ca^{2+} modification of titanium surfaces on early microbial biofilm formation, BMC Oral Health 11 (2011) http://dx.doi.org/10.1186/1472-6831-11-8.
[19] M. Gasik, L. Van Mellaert, D. Pierrot, A. Braem, D. Hofmans, E. De Waelheyns, J. Anné, M.-F. Harmand, J. Vleugels, Reduction of biofilm infection risks and promotion of osteointegration for optimized surfaces of titanium implants, Adv. Healthc. Mater. 1 (2012) 117–127.
[20] P. Innocenzi, L. Malfatti, Mesoporous thin films: properties and applications, Chem. Soc. Rev. 42 (2013) 4198–4216.
[21] C. Sanchez, C. Boissière, D. Grosso, C. Laberty, L. Nicole, Design, synthesis, and properties of inorganic and hybrid thin films having periodically organized nanoporosity, Chem. Mater. 20 (2008) 682–737.
[22] M.G. Bellino, S. Golbert, M.C. De Marzi, G.J.A.A. Soller-Illia, M.F. Desimone, Controlled adhesion and proliferation of a human osteoblastic cell line by tuning the nanoporosity of titania and silica coatings, Biomater. Sci. 1 (2013) 186–189.
[23] M.R. Parsek, P.K. Singh, Bacterial biofilms: an emerging link to disease pathogenesis, Annu. Rev. Microbiol. 57 (2003) 677–701.
[24] H. Mansouri, S.A. Alavi, M. Yari, 2nd International Conference on Chemical, Ecology and Environmental Sciences (ICCEES'2012), Singapore April 28–29, 2012.
[25] C. Boissière, D. Grosso, S. Lepoutre, L. Nicole, A.B. Bruneau, C. Sanchez, Porosity and mechanical properties of mesoporous thin films assessed by environmental ellipsometric porosimetry, Langmuir 21 (2005) 12362–12371.
[26] M. Pezzoni, R.A. Pizarro, C.S. Costa, Protective role of extracellular catalase (KatA) against UVA radiation in *Pseudomonas aeruginosa* biofilms, J. Photochem. Photobiol. B Biol. 131 (2014) 53–64.
[27] J.H. Merritt, D.E. Kadouri, G.A. O'Toole, Growing and analyzing static biofilms, Curr. Protoc. Microbiol. 1B.1 (2005) (1B.1.1-1B.1.17).
[28] M. Dubois, K.A. Gilles, J.K. Hamilton, P.A. Rebers, F. Smith, Colorimetric method for determination of sugars and related substances, Anal. Chem. 28 (1956) 350–356.
[29] O.H. Lowry, N.J. Rosebrough, A.L. Farr, R.J. Randall, Protein measurement with the folin-phenol reagents, J. Biol. Chem. 193 (1951) 265–275.
[30] G.J.A.A. Soler-Illia, P.C. Angelomé, M.C. Fuertes, A. Calvo, A. Wolosiuk, A. Zelcer, M.G. Bellino, E.D. Martínez, Mesoporous hybrid and nanocomposite thin films: a sol-gel toolbox to create nanoconfined systems with localized chemical properties, J. Sol-Gel Sci. Technol. 57 (2011) 299–312.
[31] J.G.E. Wijman, P.P.L.A. de Leeuw, R. Moezelaar, M.H. Zwietering, T. Abee, Air-liquid inferface biofilms of *Bacillus cereus*: formation, sporulation, and dispersion, Appl. Environ. Microbiol. 73 (2007) 1481–1488.
[32] H.-C. Flemming, J. Wingender, The biofilm matrix, Nat. Rev. Microbiol. 8 (2010) 623–633.
[33] R.J. Doyle, Contribution of the hydrophobic effect to microbial infection, Microbes Infect. 2 (2000) 391–400.
[34] B. Li, B.E. Logan, Bacterial adhesion to glass and metal-oxide surfaces, Colloids Surf. B 36 (2004) 81–90.
[35] L. Rizello, B. Sorce, S. Sabella, G. Vecchio, A. Galeone, V. Brunetti, R. Cingolani, P.P. Pompa, Impact of nanoscale topography on genomics and proteomics of adherent bacteria, ACS Nano 5 (2011) 1865–1876.
[36] L. Rizello, A. Galeone, G. Vecchio, V. Brunetti, P.P. Pompa, Molecular response of *Escherichia coli* adhering onto nanoscale topography, Nanoscale Res. Lett. 7 (2012) 575.
[37] C. Diaz, R.C. Salvarezza, M.A. Fernandez Lorenzo de Mele, P.L. Schilardi, Organization of *Pseudomonas fluorescens* on chemically different nano/microstructured surfaces, ACS Appl. Mater. Interfaces 2 (2010) 2530–2539.
[38] C. Hu, S. Liu, B. Li, H. Yang, C. Fan, W. Cui, Micro-/nanometer rough structure of a superhydrophobic biodegradable coating by electrospraying for initial anti-bioadhesion, Adv. Healthc. Mater. 2 (2013) 1314–1321.
[39] M.V. Roldán, P. de Oña, Y. Castro, A. Durán, P. Faccendini, C. Lagier, R. Grau, N.S. Pellegri, Photocatalytic and biocidal activities of novel coating systems of mesoporous and dense TiO_2-anatase containing silver nanoparticles, Mater. Sci. Eng. C 43 (2014) 630–640.
[40] T. Wei, Q. Yu, W. Zhan, H. Chen, A smart antibacterial surface for the on-demand killing and releasing of bacteria, Adv. Healthc. Mater. 5 (2016) 449–456.
[41] N. An, H. Lin, C. Yang, T. Zhang, R. Tong, Y. Chen, F. Qu, Gated magnetic mesoporous silica nanoparticles for intracellular enzyme-triggered drug delivery, Mater. Sci. Eng. C 69 (2016) 292–300.
[42] J. Jiao, X. Li, S. Zhang, J. Liu, D. Di, Y. Zhang, Q. Zhao, S. Wang, Redox and pH dual-responsive PEG and chitosan-conjugated hollow mesoporous silica for controlled drug release, Mater. Sci. Eng. C 67 (2016) 26–33.
[43] Pourjavadi, Z.M. Tehrani, Mesoporous silica nanoparticles with bilayer coating of poly(acrylic acid-co-itaconic acid) and human serum albumin (HSA): a pH-sensitive carrier for gemcitabine delivery, Mater. Sci. Eng. C 61 (2016) 782–790.
[44] M. Prokopowicz, K. Czarnobaj, A. Szewczyk, W. Sawicki, Preparation and in vitro characterisation of bioactive mesoporous silica microparticles for drug delivery applications, Mater. Sci. Eng. C 60 (2016) 7–18.
[45] F. Rehman, A. Rahim, C. Airoldi, P.L. Volpe, Preparation and characterization of glycidyl methacrylate organo bridges grafted mesoporous silica SBA-15 as ibuprofen and mesalamine carrier for controlled release, Mater. Sci. Eng. C 59 (2016) 970–979.